TrueCourse Biosciences

WHITEPAPER · GPCR / CRYO-EM

From Gene to Structure: Exploring MC4R in Unliganded and Ligand-Bound Conformations

A gene-to-structure case study: expression, purification and cryo-EM structure determination of the melanocortin 4 receptor–G-protein complex, with and without the agonist setmelanotide.

Catalano, C.; Byrne, S.; Haineault, J.; Fencil, K.; Mishra, A.K.; Senko, S.; Luksic, W. R.; Fisher, B.; Poweleit, N.; Muccini, A.; Scapin, G.; Gottler, L.

Introduction

G protein-coupled receptors (GPCRs) constitute the largest family of cell-surface receptors in humans, with approximately 800 members present in the human genome. They are commonly classified into six major groups: Class A (rhodopsin-like), Class B1 (secretin), Class B2 (adhesion), Class C (glutamate), Class F (Frizzled/Smoothened), and Taste2 receptors. Together, these receptors respond to a diverse range of extracellular stimuli and regulate essential physiological processes, including neuronal signaling, metabolism, and cardiovascular, immune, and endocrine functions.

Given their physiological importance, GPCRs represent one of the most extensively targeted protein families in drug discovery. A 2025 analysis by Sánchez Lorente and colleagues identified 516 approved GPCR-targeting drugs, accounting for approximately 36% of all approved drugs and acting on 121 distinct receptors.[1] Despite this therapeutic success, a substantial portion of the GPCRome remains unexplored, highlighting opportunities for the development of new therapies through structure-guided drug discovery.

Among these receptors, the melanocortin-4 receptor (MC4R), a Class A GPCR, plays a central role in regulating appetite and energy homeostasis. MC4R is expressed in several regions of the brain, including the paraventricular nucleus (PVN) of the hypothalamus, and impaired receptor signaling is associated with severe early-onset obesity.[2] Within the hypothalamic melanocortin pathway, MC4R integrates opposing neuronal signals that regulate food intake (Figure 1). Proopiomelanocortin (POMC) neurons release α- and β-melanocyte-stimulating hormones (α-MSH and β-MSH), which activate MC4R and promote satiety. In contrast, agouti-related peptide (AgRP), released by AgRP neurons, opposes receptor activation and promotes hunger.

MC4R primarily signals through Gs proteins, stimulating adenylyl cyclase and increasing intracellular cyclic AMP (cAMP) levels. However, its signaling activity extends beyond this canonical pathway, with Gq/11 coupling, β-arrestin recruitment, and receptor trafficking also contributing to its physiological responses.[2–4] Studies in mice suggest that these pathways play distinct roles in regulating food intake, energy expenditure, and cardiovascular function. MC4R activity is further modulated by accessory proteins, including melanocortin-2 receptor accessory protein 2 (MRAP2), which can influence receptor coupling, internalization, and localization to neuronal primary cilia.[4] These observations highlight the complexity of MC4R regulation, in which receptor conformation, ligand binding, and the cellular environment collectively influence signaling outcomes.

An additional feature of MC4R is its constitutive activity, which allows the receptor to signal in the absence of an agonist. Within the canonical cAMP pathway, AgRP acts as an inverse agonist, suppressing basal receptor activity in addition to antagonizing agonist-induced activation.[3] This ligand-independent signaling behavior raises important questions about the structural basis of receptor activation and how agonist binding influences receptor conformation and the stability of its associated signaling complex.

Understanding these mechanisms is particularly relevant to the development of MC4R-targeted therapies. Early agonists faced challenges related to potency, pharmacokinetics, and tolerability, emphasizing the need to understand not only ligand affinity but also the molecular mechanisms underlying receptor activation.[2–5] Setmelanotide, a clinically approved MC4R agonist, has demonstrated therapeutic benefits in selected genetic forms of obesity, with clinical studies reporting reductions in hunger and body weight.[6] Although these findings support the therapeutic potential of MC4R activation, differences in study design

and patient populations limit broader conclusions regarding its efficacy and long-term safety in general obesity.

Structural and biophysical approaches provide complementary tools for investigating the molecular interactions underlying MC4R ligand recognition. Cryo-electron microscopy (cryo-EM) enables direct visualization of receptor conformations and ligand interactions within the binding pocket, while surface plasmon resonance (SPR) provides quantitative measurements of receptor–ligand binding affinity. Together with biochemical characterization, these methods offer a way for examining how ligand binding relates to receptor structure and signaling complex stability, although the functional consequences of specific conformations require cell-based studies.

In this study, we investigated MC4R–G-protein complexes prepared in the presence and absence of setmelanotide, comparing their purification behavior, biochemical stability, and cryo-EM structures. We also characterized the binding affinity of setmelanotide for MC4R using SPR. By integrating these approaches, we aimed to better understand the molecular basis of setmelanotide recognition, its contribution to receptor–G-protein complex stability, and the structural differences between ligand-bound and unliganded MC4R.

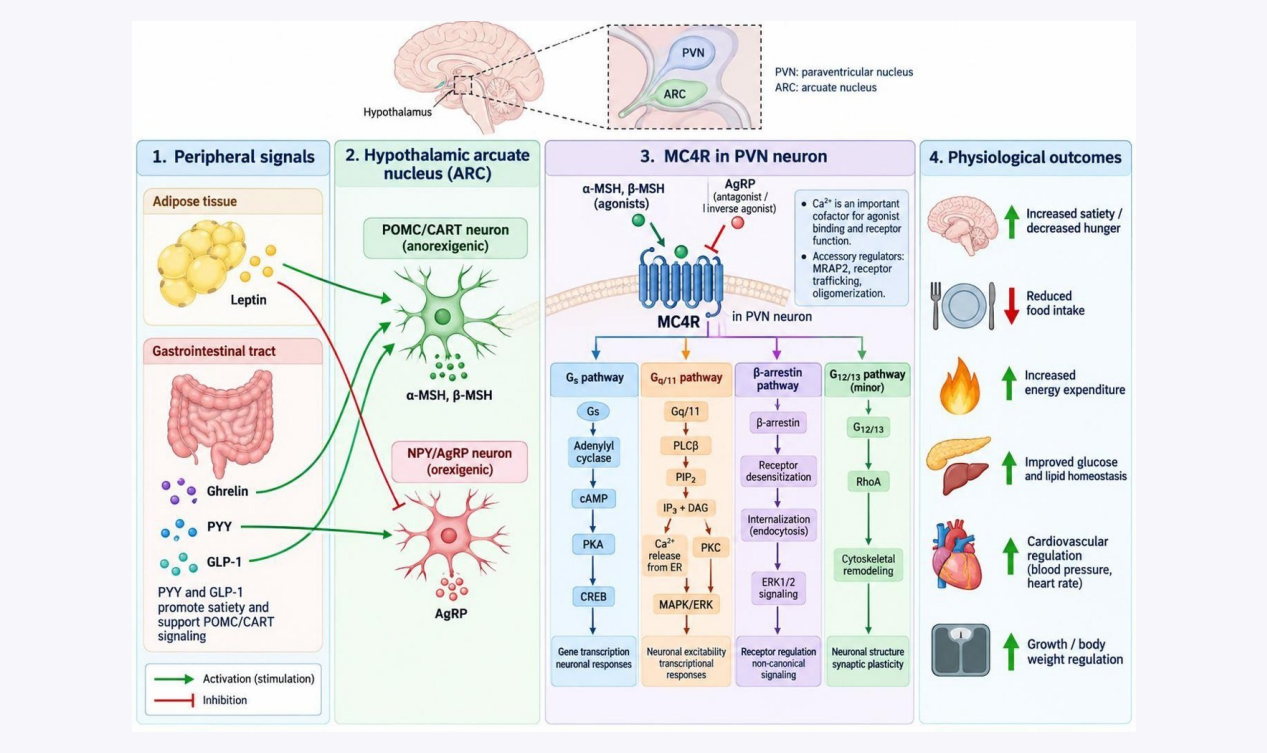


Figure 1. The melanocortin–MC4R signaling pathway. Peripheral signals influence hypothalamic POMC and AgRP neurons, which release α-/β-MSH and AgRP, respectively. MC4R integrates these inputs through several signaling pathways. Biological context is reviewed by Kühnen and colleagues[2] and Jamaluddin and colleagues.[4] Figure generated using AI.

MC4R architecture and ligand recognition

MC4R is a Class A (rhodopsin-like) GPCR characterized by seven transmembrane helices that form a ligand-binding pocket at the extracellular surface (Figure 2A). Unlike many other Class A GPCRs, MC4R has an unusually short second extracellular loop (ECL2) and lacks the conserved disulfide bridge between ECL2 and transmembrane helix 3 (TM3), contributing to the accessibility of its binding pocket to peptide ligands.[3,7] A distinctive feature of this pocket is the presence of a calcium-binding site at the TM2–TM3 interface, formed by the acidic residues E100, D122, and D126. In melanocortin peptide-bound structures, the calcium ion helps stabilize ligand recognition by coordinating both receptor residues and the peptide backbone. The coordination geometry varies among ligands, allowing the binding pocket to accommodate different peptide conformations while maintaining this key interaction.[7,8]

Melanocortin peptide recognition is largely mediated by a conserved histidine–phenylalanine–arginine–tryptophan (HFRW) pharmacophore, shared by endogenous ligands such as α-MSH and several synthetic analogues (Figure 2B–D). Within the binding pocket, the histidine residue can form a hydrogen bond with T101 while establishing hydrophobic contacts with F284 and L288. Deeper in the pocket, F261 and L265 provide hydrophobic surfaces that accommodate the aromatic portions of the ligand, whereas H264 and S188 in ECL2 contribute to hydrogen-bonding interactions around the tryptophan region. Additional polar contacts involving N123 further support ligand recognition, although their arrangement depends on the peptide conformation.[3,7,8]

Beyond these conserved interactions, the shape and flexibility of the binding pocket play an important role in determining how different ligands are accommodated and influence receptor activity. Residues I129, L133, and L197 contribute to the spatial organization of the pocket, where relatively small differences in ligand size or stereochemistry can alter local packing interactions. This is illustrated by SHU9119, a melanocortin receptor antagonist whose bulky D-naphthylalanine group interacts differently with L133 compared with the smaller phenylalanine-containing groups of related peptide agonists. Interestingly, substitution of L133 with a methionine can convert SHU9119 from an antagonist into an agonist without preventing ligand binding.[3,7,8] This example highlights how subtle changes in receptor–ligand interactions can influence ligand efficacy, even when the overall binding mode is largely preserved.

These structural features show how MC4R combines a conserved peptide recognition mechanism with sufficient binding-pocket flexibility to accommodate ligands with different pharmacological properties. Understanding these interactions provides a foundation for interpreting the binding mode of setmelanotide and the structural differences observed between the ligand-bound and unliganded MC4R complexes examined in this study.

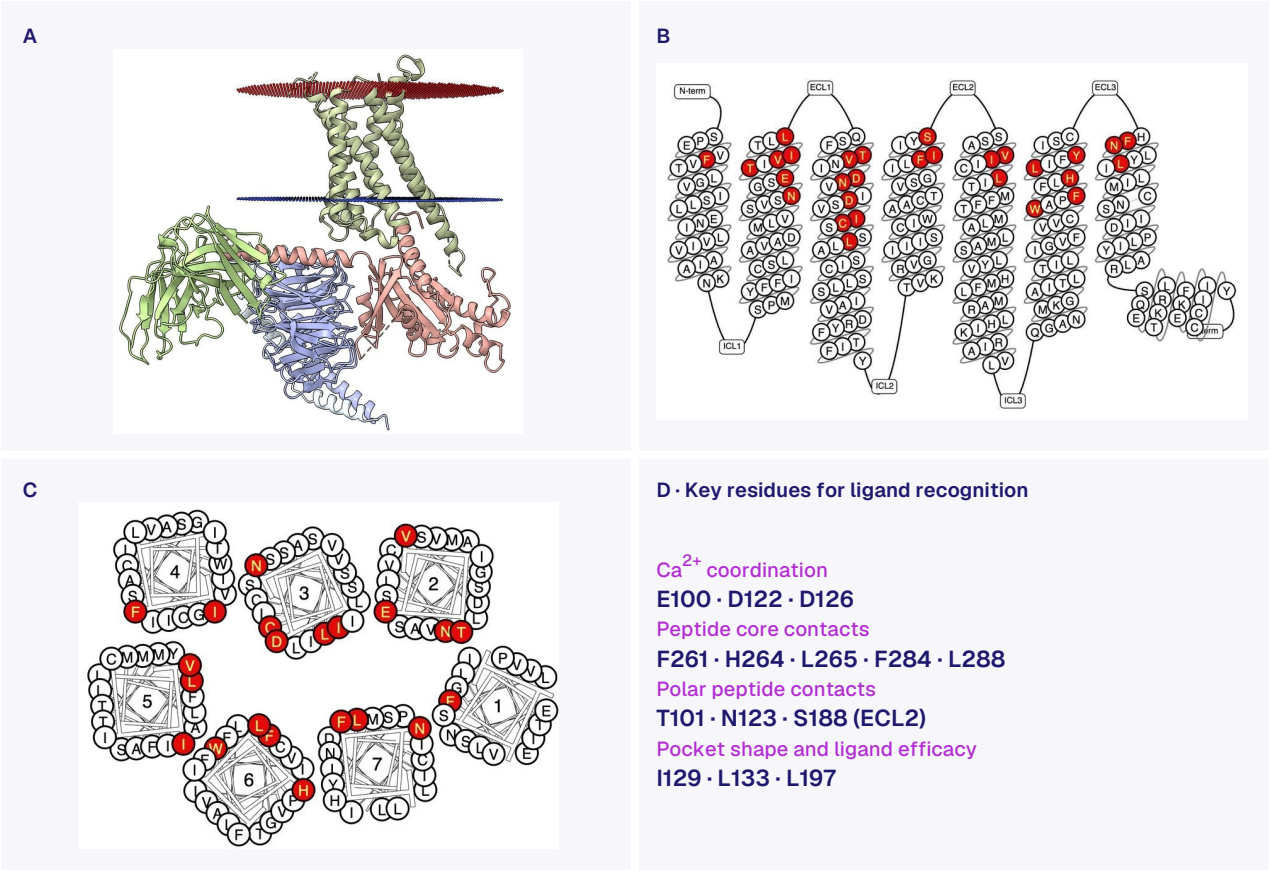


Figure 2. MC4R receptor architecture and residues involved in ligand recognition. (A) MC4R embedded in the membrane. (B, C) Helical wheel representations of the transmembrane bundle shown in two views, with key residues highlighted. Figures adapted from GPCRdb. (D) Residues grouped by their contributions to calcium coordination, peptide contacts and pocket shape; these roles can overlap. Residue annotations: GPCRdb and published MC4R structures.[7,8]

Results and Discussion

Expression and purification of the MC4R–setmelanotide complex

MC4R was co-expressed with heterotrimeric G proteins and the stabilizing antibody fragment scFv16 in *Trichoplusia ni* (Tni) insect cells. The receptor–G-protein complex was co-purified with setmelanotide, a cyclic octapeptide agonist maintained throughout the purification to stabilize the ligand-bound active state. Purification followed a four-step workflow: (1) cell lysis and membrane preparation; (2) detergent solubilization of the complex from the membrane using LMNG with CHS; (3) affinity chromatography on TALON resin; and (4) preparative size-exclusion chromatography (SEC) on Superose 6 in an LMNG/GDN/CHS formulation.

SDS-PAGE across the affinity purification shows a markedly enriched complex in the TALON pool (Figure 3A, lane 7). The preparative SEC step yielded a single dominant, symmetric peak (Figure 3B), and SDS-PAGE of the individual fractions was uniformly clean (Figure 3C). In the final concentrated pool, all components of the complex are resolved: Gα (43.0 kDa), MC4R (38.8 kDa) co-migrating with Gβ (39.4 kDa), scFv16 (28.8 kDa) and Gγ (7.7 kDa) (Figure 3D).

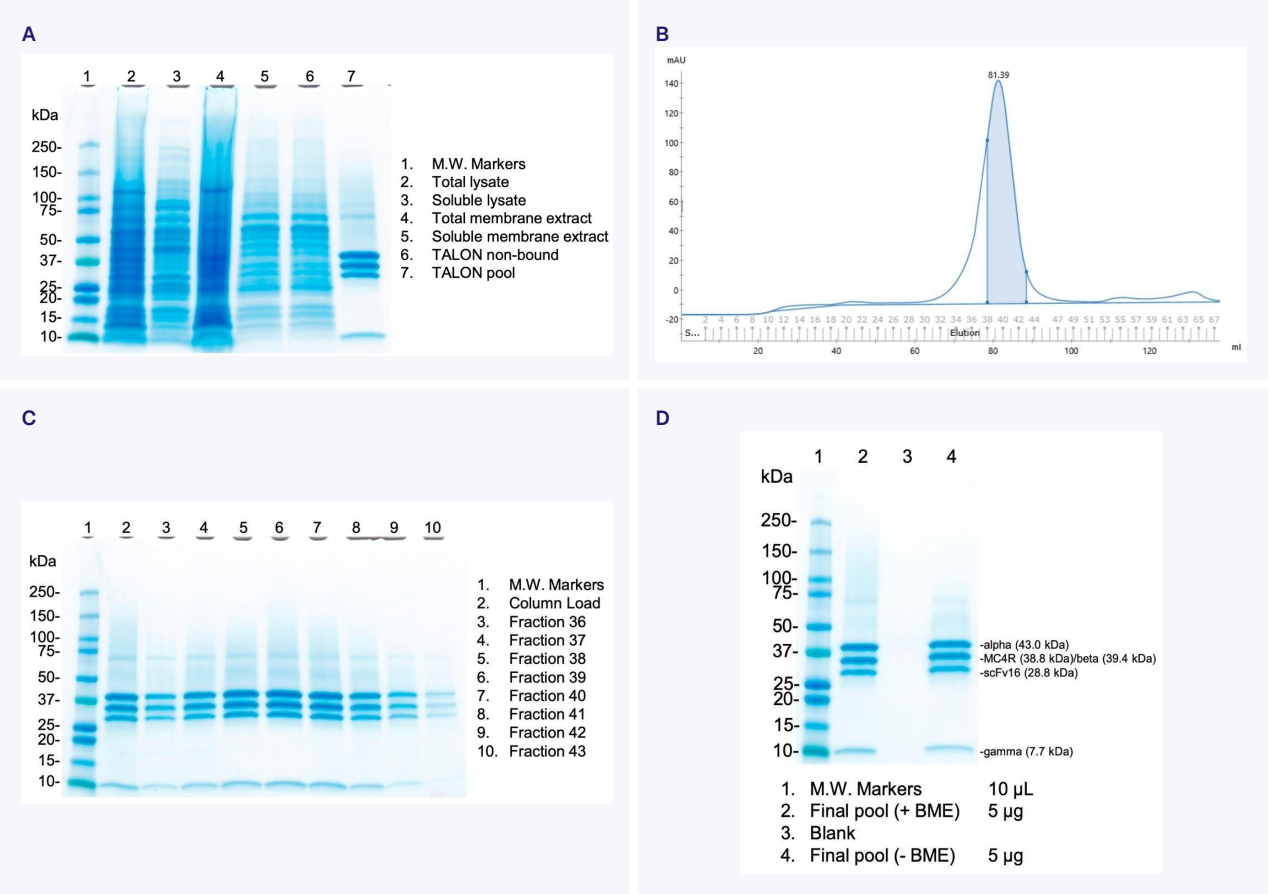


Figure 3. Purification of the MC4R–setmelanotide complex. (A) SDS-PAGE of the lysis, membrane-preparation and TALON affinity steps. (B) Preparative Superose 6 chromatogram. (C) SDS-PAGE of SEC fractions. (D) Final pool analyzed with (+BME) and without (–BME) reducing agent; all five components of the complex are present.

Expression and purification of unliganded MC4R

To investigate to which extent the agonist may contribute to the complex integrity, the same construct and steps were used in a workflow in which setmelanotide was omitted from the buffers. By every conventional purification metric, the unliganded (apo) preparation was indistinguishable from the liganded one. The affinity step gave comparable enrichment (Figure 4A), the preparative Superose 6 profile showed a single dominant peak at a similar elution volume (Figure 4B), the SEC fractions were clean (Figure 4C), and the final concentrated pool resolved all components of the complex (Figure 4D).

Standard in-process analytics, including gel purity, chromatographic profile and yield, reported a well-behaved sample in both cases.

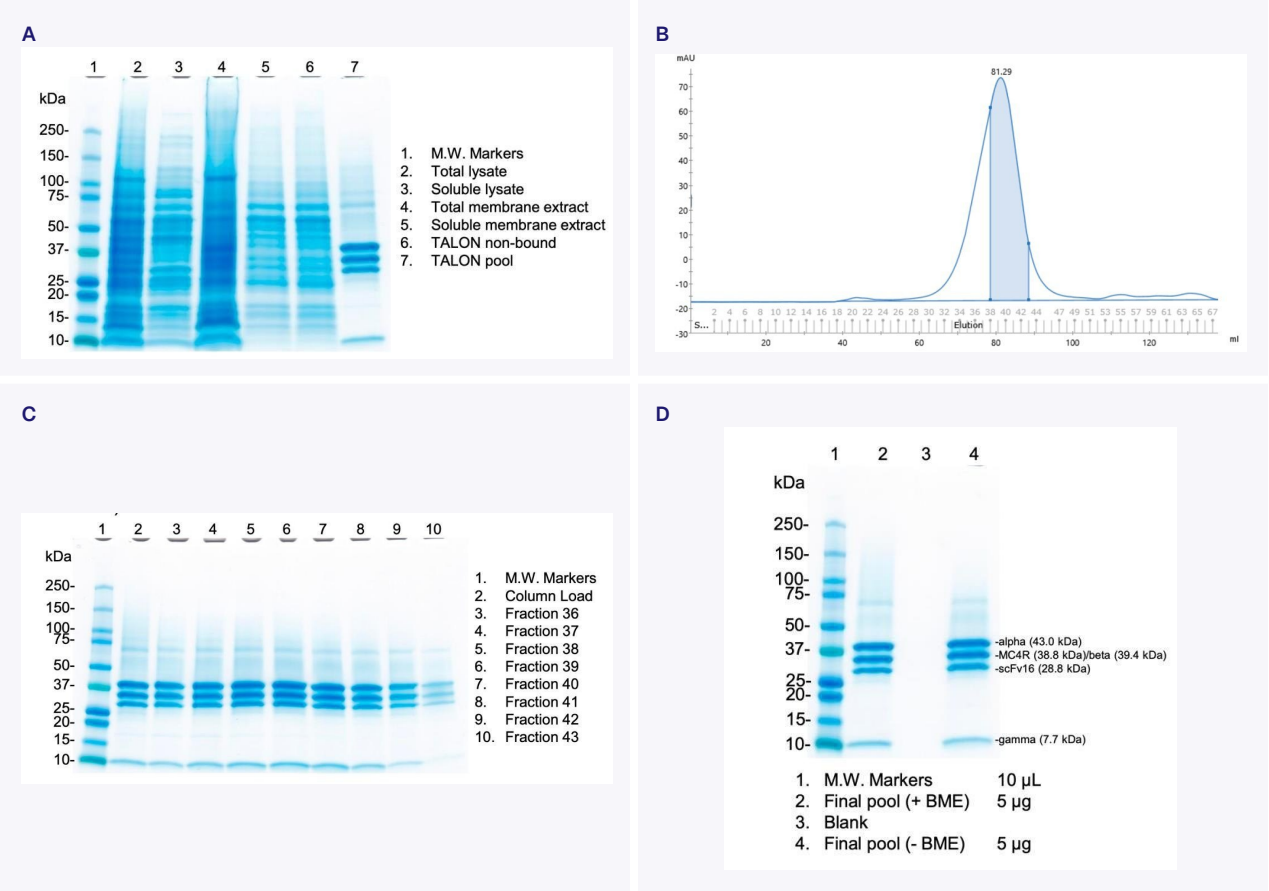


Figure 4. Purification of the unliganded MC4R complex. (A) Lysis, membrane-preparation and TALON affinity steps. (B) Preparative Superose 6 chromatogram. (C) SDS-PAGE of SEC fractions. (D) Final pool ±BME. The profiles closely match those of the setmelanotide-bound preparation in Figure 3.

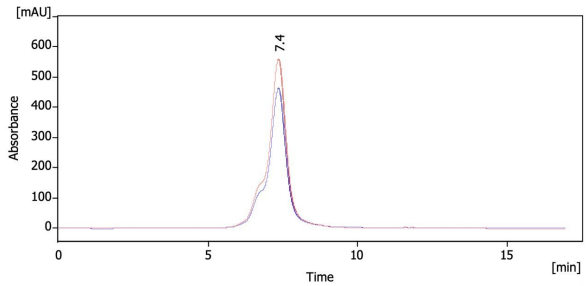
Freeze–thaw stability and negative-stain screening

Analytical SEC was subsequently used to probe the stability of each complex before and after a freeze–thaw cycle. The setmelanotide-bound complex eluted as a single peak and was essentially unchanged by freezing (Figure 5A).

The apo complex behaved differently. A second peak accounted for roughly half the integrated area and was already present immediately after preparative SEC, before freezing (Figure 5B). This supports a stabilizing role for setmelanotide under the conditions tested. These behaviors were confirmed through negative-stain analysis of the complexes. The liganded sample was homogeneous and we were able to obtain 2D class averages showing the intact complex, with the micelle and heterotrimer clearly resolved (Figure 5C). The apo sample contained a large population of smaller particles consistent with dissociation, and we were not able to obtain interpretable 2D classes (Figure 5D).

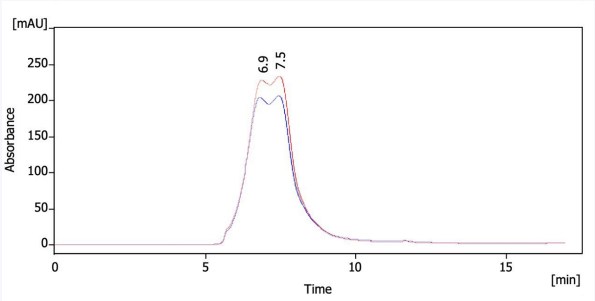
Instability increased during cryo-EM preparation: after a second freeze–thaw cycle, nearly all of the apo complex had dissociated.

A · Setmelanotide



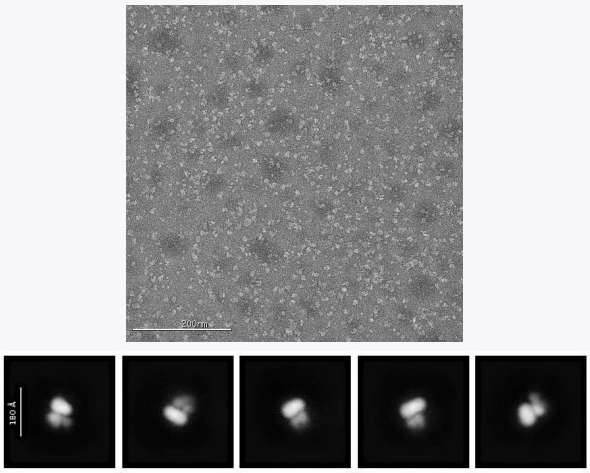
Samples	Peak #	Peak Retention time (min)	Area (mAU)	Area (%)
Pre-Freeze/thaw	1	7.4	20658.1	100.0
	Total		20658.1	100.0
Post-Freeze/thaw	1	7.4	25168.1	100.0
	Total		25168.1	100.0

B · Unliganded



Samples	Peak #	Peak Retention time (min)	Area (mAU)	Area (%)
Pre-Freeze/thaw	1	6.8	10254.2	46.5
	2	7.5	11781.2	53.5
	Total		22035.4	100.0
Post-Freeze/thaw	1	6.9	11526.5	47.3
	2	7.5	12828.5	52.7
	Total		24355.0	100.0

C · Setmelanotide



D · Unliganded

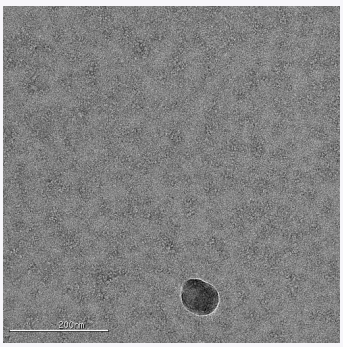


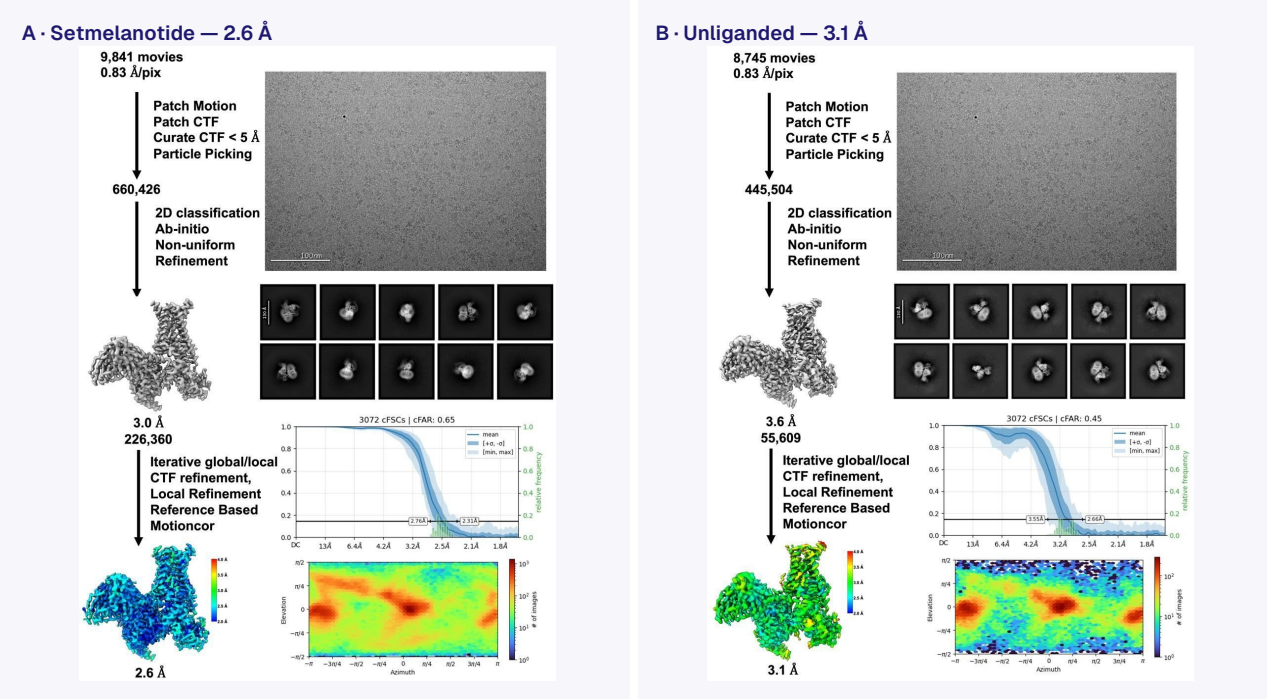
Figure 5. Sample quality. (A, B) Analytical SEC pre- and post-freeze–thaw for the setmelanotide-bound and unliganded complexes, with peak integration. (C, D) Representative negative-stain micrographs and 2D class averages for the setmelanotide complex.

Structure determination of MC4R in complex with setmelanotide and unliganded

Despite the instability observed for the unliganded sample, both preparations were used for cryo-EM analysis. The samples were vitrified without further dilution on glow-discharged UltrAuFoil 1.2/1.3 grids. Data were collected on a Titan Krios transmission electron microscope at a pixel size of 0.83 Å. Data processing followed a standard single-particle analysis workflow,[9] as summarized in Figure 6.

For the 3D structure of MC4R bound to setmelanotide, a total of 9,841 manually curated micrographs were used for particle picking, resulting in 660,426 particles. The initial 2D classification showed well-defined classes with visible secondary structure features, including the G-protein heterotrimer and the transmembrane helical bundle of MC4R surrounded by the detergent micelle. Following iterative rounds of 2D and 3D classification, an initial reconstruction at 3.0 Å was obtained using 226,360 particles. Further refinement improved the nominal resolution to 2.6 Å (Figure 6A). A subset of particles yielded a reconstruction at 2.3 Å; however, the 2.6 Å map was selected for model building, as it showed better-defined density for the bound agonist and several solvent-exposed side chains.

For the unliganded sample, a total of 8,745 movies were collected, yielding 445,504 particles. Following 2D and 3D classification, only 55,609 particles contributed to the final reconstruction at a nominal resolution of 3.1 Å (Figure 6B). Analysis of the particle populations revealed that more than 60% of the dataset consisted of dissociated species. Several 2D classes initially resembling top views of the intact complex were identified as free G-protein heterotrimers. These observations are consistent with the analytical SEC and negative-stain EM results, which suggested reduced stability of the unliganded complex compared to the setmelanotide-bound sample.



MOVIES COLLECTED **9,841 / 8,745**	PIXEL SIZE **0.83 Å**	PARTICLES PICKED **660,426 / 445,504**
PARTICLES IN FINAL MAP **226,360 / 55,609**	GRID TYPE **UltrAuFoil 1.2/1.3**	FINAL RESOLUTION **2.6 Å / 3.1 Å**

Figure 6. Cryo-EM data processing. (A) Setmelanotide-bound complex. (B) Unliganded complex. Each panel shows a representative micrograph, 2D class averages, the FSC curve, the local-resolution-coloured map and the angular distribution. Table values are given as setmelanotide / unliganded. EMDBs: EMD-79944 and EMD-79943.

The MC4R–setmelanotide–G-protein complex

Setmelanotide is a cyclic octapeptide characterized by an intramolecular disulfide bond between Cys2 and Cys8, which constrains the conformation of the pharmacophore involved in receptor recognition. The MC4R–setmelanotide complex was reconstructed by cryo-EM at a nominal resolution of 2.6 Å, allowing visualization of the complete signaling assembly, including MC4R, the Gα, Gβ1, and Gγ2 subunits of the heterotrimeric G protein, the stabilizing scFv16, the bound setmelanotide peptide, and a coordinated calcium ion (Figure 7).

The cryo-EM map revealed well-defined density for setmelanotide within the orthosteric binding pocket formed by the extracellular portions of the MC4R transmembrane helices, with the second extracellular loop (ECL2) positioned above the peptide. In particular, the side chains of the tryptophan, phenylalanine,

and histidine residues comprising the core pharmacophore were clearly resolved, enabling detailed characterization of their interactions with the receptor. Although some solvent-exposed regions of the peptide exhibited less well-defined density, consistent with increased conformational flexibility, sufficient density was present to model Arg1 and fit the complete peptide into the binding pocket.

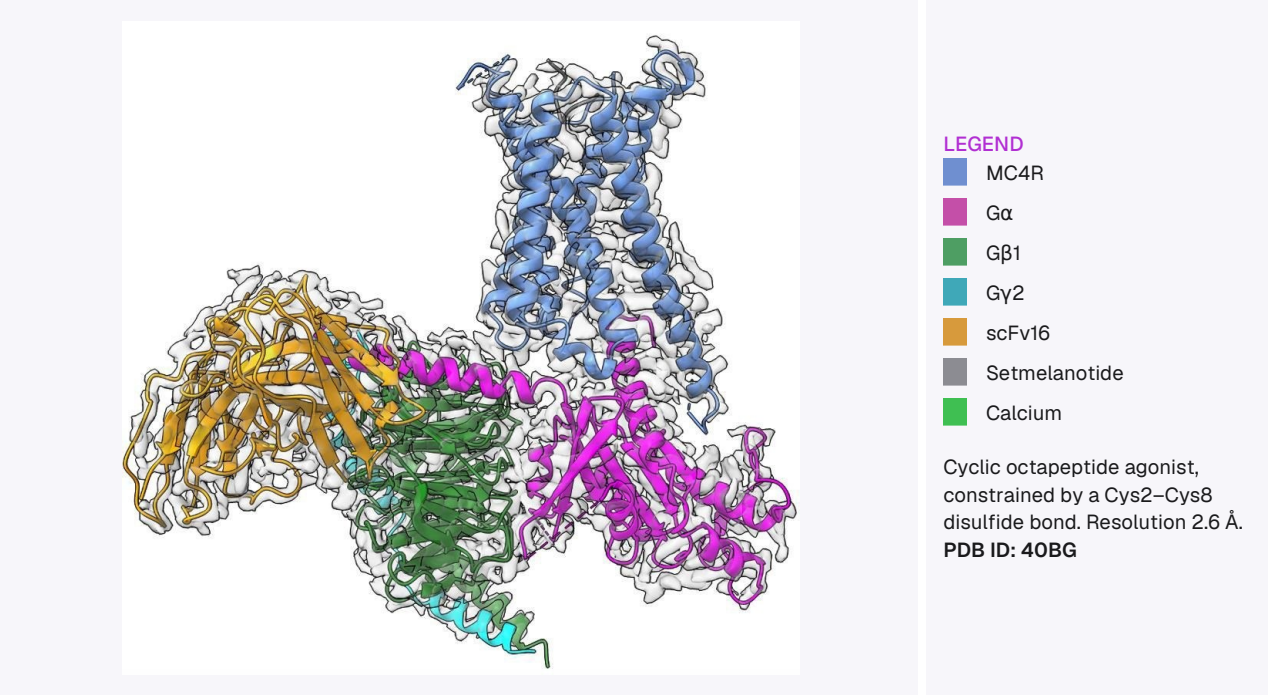
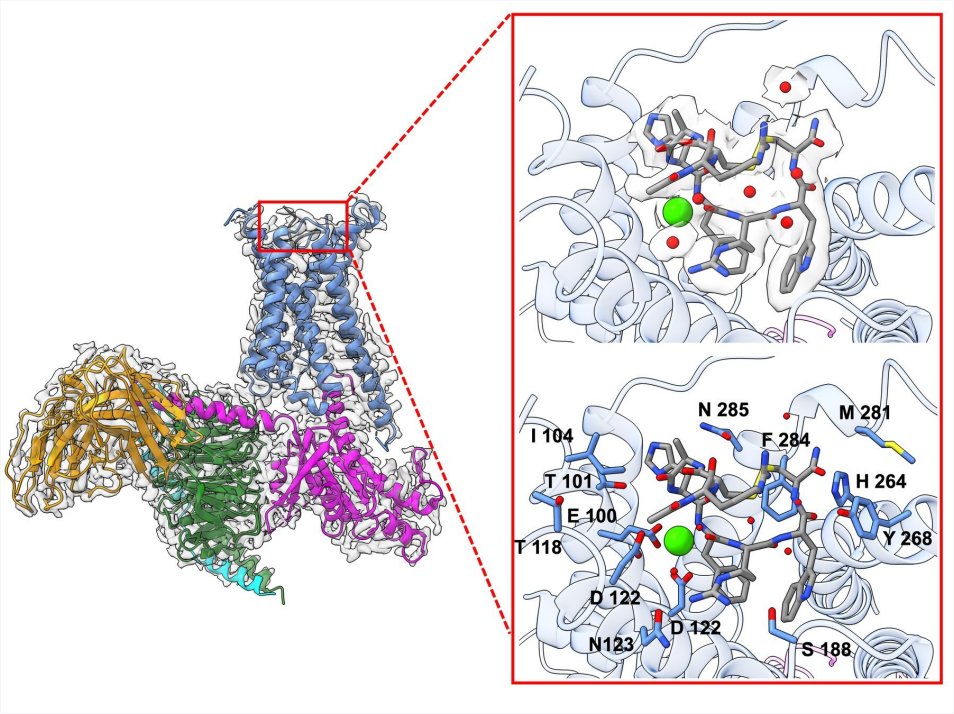


Figure 7. Cryo-EM structure of the MC4R–setmelanotide complex, with the model fitted into the density. The receptor is shown at the top with the G-protein heterotrimer and scFv16 below. Rendered with UCSF ChimeraX.[10]

Closer inspection of the binding site revealed an extensive network of interactions contributing to setmelanotide recognition and stabilization (Figure 8). A calcium ion was identified at the base of the orthosteric pocket, coordinated by E100, D122, and D126 of MC4R, together with backbone atoms of setmelanotide. This coordination establishes a bridge between the receptor and the peptide, highlighting the important role of calcium in melanocortin ligand recognition.[7,8] In addition, several ordered water molecules were modeled within the binding pocket, forming a potential solvent-mediated interaction network surrounding the bound peptide. These include water molecules positioned near the calcium coordination site and along the peptide–receptor interface, as well as a water molecule near S282. Their distribution suggests that water-mediated interactions may contribute to the organization of the binding pocket and stabilization of the ligand-binding environment. Additional interactions involve S188 in ECL2, which forms a hydrogen bond with the peptide backbone, helping to position the extracellular loop over the bound ligand. The aromatic residues F284, H264, and Y268 also interact with the hydrophobic and aromatic portions of setmelanotide, further supporting the positioning of the core pharmacophore within the binding pocket.

The overall binding mode observed in our structure is in good agreement with the previously published MC4R–setmelanotide complex (PDB ID: 7PIU).[8] Structural differences are primarily localized to solvent-exposed regions of the peptide, where increased flexibility can accommodate alternative side-chain conformations. Arg1 adopts a different rotamer compared with the published structure, although this variation does not substantially alter the overall binding pose of setmelanotide.



CALCIUM BRIDGE

E100 and D126 chelate Ca^{2+}, which also contacts the setmelanotide backbone.

ECL2 CLOSURE

S188 hydrogen-bonds to the peptide backbone; ECL2 folds toward the pocket.

AGREEMENT WITH 7PIU

Differences are limited to solvent-exposed side chains such as Arg1.

Figure 8. The setmelanotide binding site. The boxed region of the complex (left) is enlarged at right: the top panel shows density for each residue of the cyclic octapeptide and for the coordinated calcium ion, and the bottom panel labels the surrounding receptor residues. Rendered with UCSF ChimeraX.[10]

Structural comparison between unliganded and setmelanotide-bound MC4R

Structural superposition of MC4R in its setmelanotide-bound (PDB ID: 40BG) and unliganded states (PDB ID: 40BF) revealed an overall highly conserved receptor conformation, with a Cα RMSD of 0.6 Å (Figure 9A). Despite this close structural agreement, several local differences were identified within the orthosteric binding pocket, particularly in regions involved in ligand recognition, calcium coordination, and extracellular loop organization.

Several structural differences were observed around the calcium-binding site. In the setmelanotide-bound structure, a well-defined calcium ion was identified within the orthosteric pocket, coordinated by E100, D122, and D126, together with backbone atoms of setmelanotide. Several ordered water molecules were also modeled in this region, suggesting a potential contribution of solvent-mediated interactions to the organization of the ligand-binding environment. In contrast, no equivalent calcium density could be confidently identified in the unliganded reconstruction, and the surrounding binding pocket displayed local conformational rearrangements. E100 underwent a positional shift accompanied by partial unwinding of the adjacent helical segment, while D126 adopted a different side-chain orientation. Changes were also observed in the organization of the second extracellular loop (ECL2), which moved away from the position it had in the setmelanotide-bound structure (Figure 9B,C). These differences indicate that the local architecture of the calcium-binding region and the surrounding extracellular pocket is dependent on the

presence or absence of a bound molecule.

The lack of well-defined calcium density in the unliganded reconstruction, however, does not necessarily indicate that calcium is absent or unable to bind under these conditions. Differences in local flexibility, ion occupancy, and map resolution may influence the visibility of individual ions and solvent molecules. Similarly, the absence of a clearly resolved water network in the unliganded pocket should not be interpreted as evidence that these interactions are entirely absent. Although the structural comparison highlights changes in the calcium coordination environment and the organization of the orthosteric pocket, the contribution of these differences to constitutive MC4R signaling remains uncertain. Previous studies have not established whether calcium occupancy is required for basal receptor activity.[4] Additional biophysical and functional experiments would therefore be necessary to determine how calcium coordination, local hydration, and ligand-dependent conformational changes influence MC4R activation.

In the unliganded reconstruction we also identified some additional density within the orthosteric binding pocket. This density could not be confidently assigned to protein residues or possible ligands and was therefore not modeled. One possible explanation for the residual density is the involvement of the MC4R N-terminal region in receptor autoactivation, as previously proposed by Kleinau and colleagues.[3] Compared with the setmelanotide-bound structure, approximately seven residues of the N-terminal region could not be modeled in the unliganded reconstruction due to insufficiently defined density. This observation raises the possibility that the flexible N-terminal segment contributes to the unidentified density within the binding pocket. Alternatively, the density may originate from detergent or lipid molecules retained during purification. Similar unassigned densities have been reported by Feng and colleagues in structures of unliganded melanocortin receptors.[11] Therefore, although no exogenous agonist was added during preparation of the unliganded complex, the identity of the additional density remains uncertain and cannot be confidently attributed to a specific molecular component based on the current reconstruction.

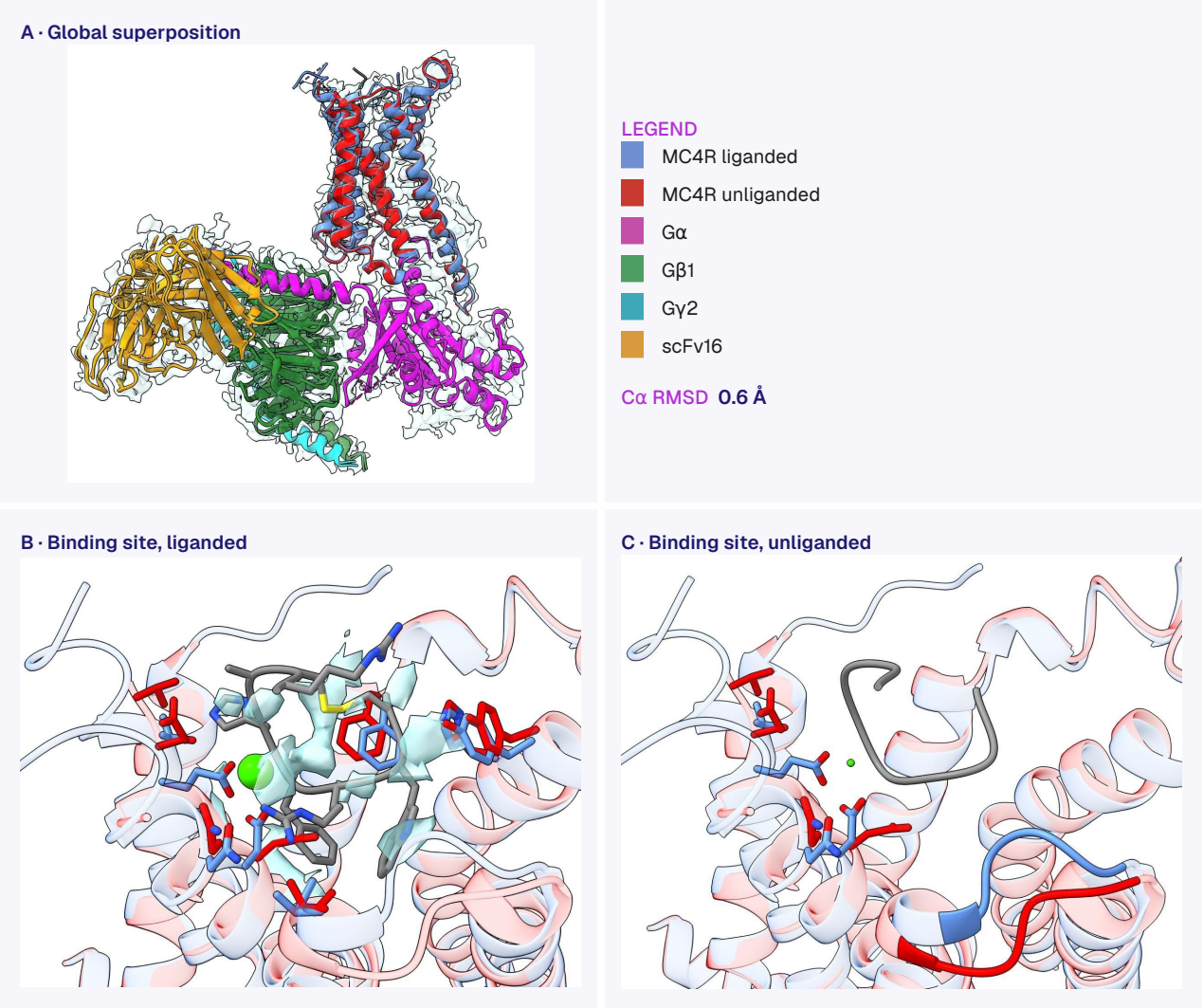


Figure 9. Comparison of the liganded and unliganded receptors. (A) Superposition of the two complexes. (B, C) The orthosteric pocket in each preparation; E100 and D126 change position, the helix adjacent to E100 partially unwinds, and ECL2 rearranges. The density in the unliganded pocket remains unassigned. Rendered with UCSF ChimeraX.[10]

Surface plasmon resonance analysis of MC4R–setmelanotide binding

Surface plasmon resonance (SPR) was used to measure the affinity of setmelanotide for a purified His-tagged MC4R signaling complex comprising MC4R, heterotrimeric Gs protein, and the stabilizing antibody fragment scFv16. Experiments were performed on a Biacore 1K instrument using an anti-His antibody immobilized by amine coupling on a CM5 sensor chip. His-tagged MC4R was captured and subsequently crosslinked to stabilize surface attachment, yielding a receptor surface density of approximately 800 RU. Setmelanotide was injected as a seven-point, three-fold dilution series ranging from 20 nM to 0.027 nM in a detergent-containing running buffer using a single-cycle kinetics protocol at a flow rate of 30 µL/min, with a 120 s association phase for each concentration followed by a final 600 s dissociation phase. Sensorgrams were processed by double-reference subtraction, and steady-state binding responses were fitted to a 1:1 Langmuir binding isotherm to estimate the equilibrium dissociation constant (K_D). Because the experimental design was optimized for steady-state affinity determination, kinetic rate constants (k_{on} and k_{off}) were not extracted from these measurements.

The representative concentration–response curve showed saturable binding with an estimated equilibrium dissociation constant (K_D) of 0.24 nM (Figure 10A). Across five SPR measurements, the mean K_D was 0.21 ± 0.09 nM (Figure 10B), indicating reproducible sub-nanomolar affinity under these assay conditions. The individual affinity estimates varied moderately between measurements, but all remained within the sub-nanomolar range. The measured affinity is consistent with stable occupation of the orthosteric site in the ligand-bound sample, although it does not by itself establish the mechanism of G-protein-complex stabilization observed in the biochemical experiments.

Published studies likewise establish setmelanotide as a high-affinity MC4R agonist. A commonly reported competitive binding inhibition constant is K_i = 2.1 nM, compared with K_i ≈ 41–51 nM reported for endogenous α-MSH in particular binding assays.[8,12,13] Setmelanotide also exhibits potent MC4R-mediated cAMP signaling, with a published EC_{50} of approximately 0.27 nM.[12] Our SPR-derived K_D is lower than the reported K_i, but these values arise from different measurement principles: SPR evaluates binding to immobilized, purified receptor complex in detergent, whereas competition assays measure displacement of a tracer in a receptor-containing biological preparation. Likewise, a functional EC_{50} describes signaling potency rather than direct affinity. Consequently, the numerical differences should not be interpreted as evidence for greater intrinsic affinity or signaling efficacy in our preparation without matched-assay experiments.

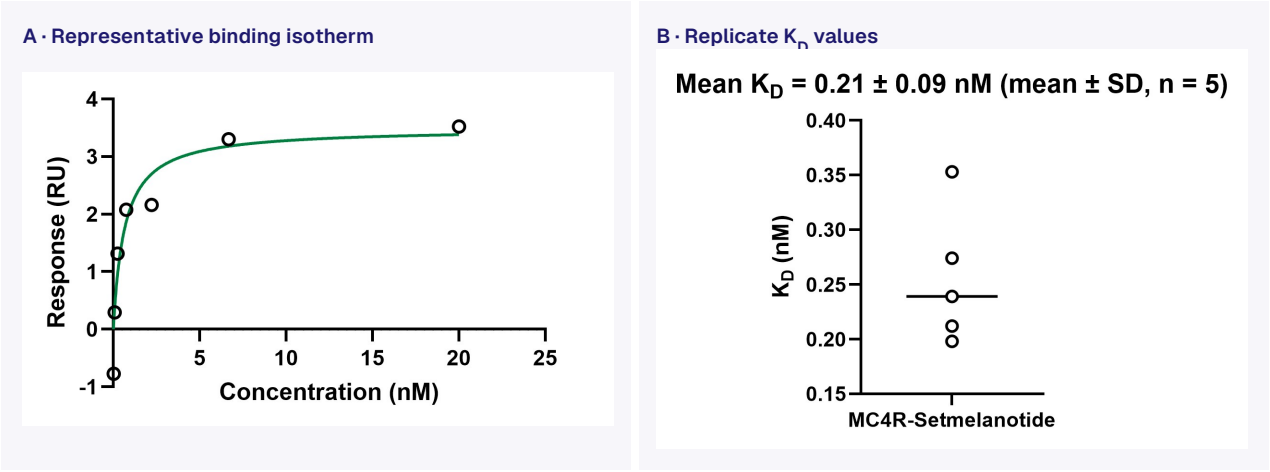


Figure 10. SPR characterization of setmelanotide binding to MC4R. (A) Representative concentration-dependent steady-state response and 1:1 binding fit (K_D = 0.24 nM). (B) Distribution of affinity estimates from five measurements, with mean K_D = 0.21 ± 0.09 nM.

Conclusions

We determined cryo-EM structures of the MC4R–G-protein complex in presence of setmelanotide and without any added agonist at nominal resolutions of 2.6 Å and 3.1 Å, respectively. Although both preparations followed the same expression and purification workflow, they differed in complex stability. The setmelanotide-bound preparation remained homogeneous after freeze–thaw, whereas the unliganded complex showed evidence of dissociation in the preparative SEC and deteriorated further upon freezing. These differences were not apparent from an initial analysis; analytical SEC and negative-stain screening were essential for identifying them before high-resolution data collection.

This difference in sample quality was reflected in the cryo-EM analysis: only 55,609 of the 445,504 initially picked particles contributed to the final unliganded 3D reconstruction. Despite the reduced population of intact complexes, both structures could be determined. The setmelanotide-bound model closely agrees with the published structure (PDB ID 7PIU),[8] while the unliganded reconstruction complements earlier structural work on the constitutive activity of melanocortin receptors.[11] Their comparison reveals local rearrangements in the orthosteric pocket, including changes around Glu100, Asp126, and the ECL2. Additional density in the unliganded pocket remains unassigned, and the absence of a resolved calcium ion cannot be taken as evidence that calcium does not bind in this state. The potential contributions of the MC4R N-terminus and calcium to basal signaling therefore remain open questions.[3,4]

SPR analysis quantified setmelanotide binding to the purified MC4R-Gs-scFv16 complex, yielding a mean equilibrium dissociation constant (K_D) of 0.21 ± 0.09 nM across five measurements. This high-affinity interaction complements the 2.6 Å cryo-EM structure, which defines the bound peptide conformation and its calcium-associated interactions within the receptor pocket. Together, these data demonstrate stable setmelanotide engagement of the purified MC4R signaling complex under the conditions used for structural analysis.

Our study illustrates the value of integrating biochemical quality control, direct binding measurements, and high-resolution structural analysis in a gene-to-structure workflow. These approaches provide complementary views of MC4R ligand recognition and sample integrity, but neither binding affinity nor structural differences alone establish the functional consequences for receptor activation. Further biophysical and cellular studies will be needed to determine how calcium coordination, ligand occupancy, and the observed conformational changes influence MC4R signaling and therapeutic responses.[2–6]

References

1. Sánchez Lorente, J., Sokolov, A. V., Ferguson, G., Schiöth, H. B., Hauser, A. S. & Gloriam, D. E. GPCR drug discovery: new agents, targets and indications. Nat. Rev. Drug Discov. 24, 458–479 (2025). doi: 10.1038/s41573-025-01139-y
2. Kühnen, P., Krude, H. & Biebermann, H. Melanocortin-4 receptor signalling: importance for weight regulation and obesity treatment. Trends Mol. Med. 25, 136–148 (2019). doi: 10.1016/j.molmed.2018.12.002
3. Kleinau, G., Heyder, N. A., Tao, Y.-X. & Scheerer, P. Structural complexity and plasticity of signaling regulation at the melanocortin-4 receptor. Int. J. Mol. Sci. 21, 5728 (2020). doi: 10.3390/ijms21165728
4. Jamaluddin, A., McClellan, A., Raffan, E. & Gorvin, C. M. The role of accessory proteins and co-factors in regulation of melanocortin-4 receptor signalling: an update. J. Neuroendocrinol. 38, e70160 (2026). doi: 10.1111/jne.70160
5. Prindle, C. R. et al. The melanocortin receptors as targets for general obesity: contextualizing clinical failures and analyzing future perspectives. Front. Endocrinol. 17, 1797586 (2026). doi: 10.3389/fendo.2026.1797586
6. Sun, Y., Abed, M. & Sohouli, M. H. The effect of melanocortin-4 receptor agonist drugs on obesity and metabolic risk factors: a systematic review and meta-analysis. Diabetol. Metab. Syndr. 18, 40 (2026). doi: 10.1186/s13098-025-02071-2
7. Yu, J. et al. Determination of the melanocortin-4 receptor structure identifies Ca^{2+} as a cofactor for ligand binding. Science 368, 428–433 (2020). doi: 10.1126/science.aaz8995
8. Heyder, N. A. et al. Structures of active melanocortin-4 receptor–Gs-protein complexes with NDP-α-MSH and setmelanotide. Cell Res. 31, 1176–1189 (2021). PDB ID 7PIU. doi: 10.1038/s41422-021-00569-8
9. C. Catalano; K. W. Lucier; S. Senko; N. L. Tran; A. C. Farwell; S. M. Silva; P. V. Dip; N. Poweleit; G. Scapin The CryoEM structure of human serum albumin in complex with ligands. J. Struct. Biol. 2024. doi: 10.1016/j.jsb.2024.10810
10. Goddard, T. D. et al. UCSF ChimeraX: meeting modern challenges in visualization and analysis. Protein Sci. 27, 14–25 (2018). doi: 10.1002/pro.3235

11. Feng, W., Zhou, Q., Zheng, C., Yang, D. & Wang, M.-W. Structural basis for the constitutive activity of the melanocortin receptor family. Structure 33, 1074–1087.e5 (2025). doi: 10.1016/j.str.2025.03.004

12. Collet, T.-H. et al. Evaluation of a melanocortin-4 receptor (MC4R) agonist (setmelanotide) in MC4R deficiency. Mol. Metab. 6, 1321–1329 (2017). doi: 10.1016/j.molmet.2017.06.015.

13. Sharma, S. et al. Current mechanistic and pharmacodynamic understanding of melanocortin-4 receptor activation. Molecules 24, 1892 (2019). doi: 10.3390/molecules24101892.

TrueCourse Biosciences

From gene to structure, under one roof.

For more information, or to speak to one of our structural biology experts, email us at info@truecoursebio.com.

truecoursebio.com